

# Hexagonal Stacking Faults Act as Hole-Blocking Layers in Lead Halide Perovskites

Ji-Sang Park, Zhenzhu Li, Jacob N. Wilson, Wan-Jian Yin, and Aron Walsh\*



Cite This: *ACS Energy Lett.* 2020, 5, 2231–2233



Read Online

ACCESS |



Metrics & More



Article Recommendations

**ABSTRACT:** The transformation between black (corner sharing) and yellow (face sharing) polytypes of lead halide perovskites is a major performance bottleneck. We investigate phase intermixing through the simulation of stacking faults (nanodomains) that reveal a small thermodynamic cost but large electronic consequences in  $\text{CsPbI}_3$ .



The close competition between cubic-close packing (ABC) and hexagonal-close packing (AB) of elemental solids extends to crystals containing more than one element. In semiconductor physics, the cubic zincblende and hexagonal wurtzite polytypes both play important roles, and this extends to ternary and quaternary compounds.<sup>1</sup> Because of the small energy differences involved, stacking faults often emerge (e.g., AB sequences in an ABC structure) and can be found in thin-film photovoltaics such as  $\text{CdTe}$ .<sup>2</sup>

In metal halide perovskites, polytypes also play a key role as evidenced by the close competition between black (3C) and yellow (2H) phases for many compositions.<sup>3,4</sup> One distinction is that the ions in both zincblende and wurtzite maintain roughly tetrahedral coordination, while in perovskites the change in stacking sequence is associated with a transition from corner-sharing to face-sharing octahedral networks as illustrated in Figure 1. It has been established that the nanostructure of halide perovskites is nuanced with reports of local symmetry breaking, strain gradients, twin boundaries, and phase coexistence.<sup>5,6</sup>

We consider  $\text{CsPbI}_3$  in four structures. Ramsdell notation (e.g., 11H) becomes ambiguous for complex stacking sequences, so we instead describe them according to whether each halide layer is corner or face-sharing (e.g., 3c8h) as illustrated in Figure 1. Each model was optimized with density functional theory (DFT/PBESol)<sup>7,8</sup> including scalar relativistic effects using the technical setup reported elsewhere.<sup>9</sup> The spread in formation enthalpies is small (<20 meV/atom) and comparable to thermal energy at room temperature. The 2H structure is most stable for  $\text{CsPbI}_3$  in our athermal calculations, consistent with other reports.<sup>10,11</sup> Taking into account the revised ionic radii,<sup>12</sup> the Goldschmidt tolerance factor of this iodide (0.89) is less than ideal.

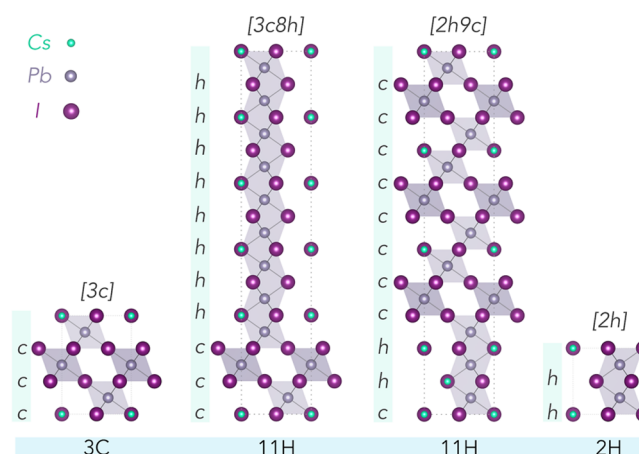


**Figure 1.** Illustration of four polytypes for  $\text{CsPbI}_3$ . The traditional cubic perovskite (3C) consists of corner-sharing  $\text{PbI}_6$  octahedra. In contrast, a face-sharing octahedral network is formed in the hexagonal (2H) structure. Two 11H polytypes are shown, which can be distinguished according to the iodine in each layer being corner-sharing (c) or face-sharing (h). Note that the stacking axis corresponds to the  $\langle 111 \rangle$  direction for a cubic perovskite unit cell.

Received: May 21, 2020

Accepted: June 5, 2020

Published: June 5, 2020



Table 1. Properties of CsPbI<sub>3</sub> with Corner-Sharing, Face-Sharing, and Mixed Stacking Sequences<sup>a</sup>

stacking	<i>a</i> (Å)	<i>c</i> (Å)	$\Delta H_f$	SFE	VBO	CBO	$E_g$ (I)
2H (2 <i>h</i> )	8.42	6.57	0				2.56 (1.86)
11H (3 <i>c</i> 8 <i>h</i> )	8.49	41.98	6	0.11	−0.12	−0.07	2.10 (1.81)
11H (2 <i>h</i> 9 <i>c</i> )	8.72	40.96	15	0.07	−0.26	0.00	1.44
3C (3 <i>c</i> )	8.83	10.81	18				1.18

<sup>a</sup>The formation enthalpy ( $\Delta H_f$ ) is given with respect to the lowest-energy polymorph (meV/atom). The stacking fault energy (SFE) is given in eV/nm<sup>2</sup>. The valence and conduction band offsets (VBO/CBO) are given in eV.  $E_g$  refers to the direct (and indirect, I) band gap in eV. Note that band gaps are underestimated at this level of theory (DFT/PBESol).

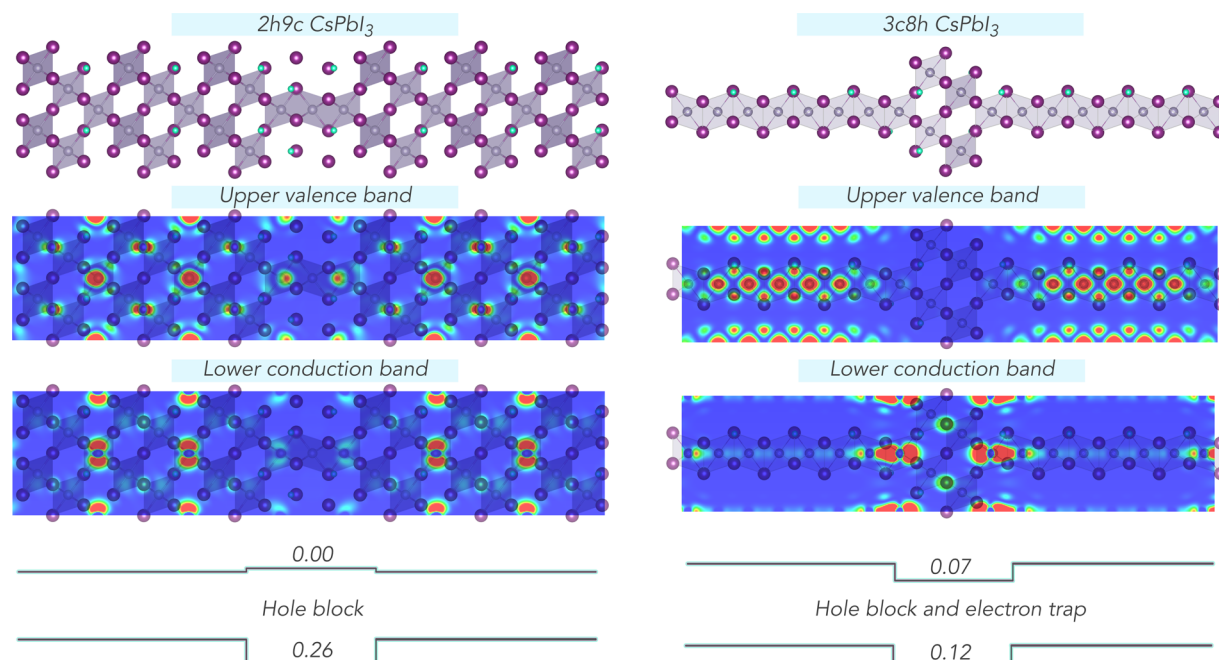


Figure 2. Electron density distribution associated with the highest occupied and lowest unoccupied crystal orbitals for stacking faults in CsPbI<sub>3</sub>. The electron density is plotted through a (100) slice containing Pb and I atoms from blue (zero density) to red (high density).

We define an effective stacking fault energy (SFE) that describes the miscibility of corner and face-sharing regions as

$$\text{SFE}_{\text{NcMh}} = \frac{1}{A} \left( E_{\text{NcMh}} - \frac{N}{3} E_{3c} - \frac{M}{2} E_{2h} \right) \quad (1)$$

$E$  represents the DFT total energy, and  $N$  and  $M$  are the number of corner-sharing and face-sharing layers, respectively. The corresponding values are listed in Table 1. The cubic fault in a hexagonal structure has a cost of 0.11 eV/nm<sup>2</sup>, which is lower than that of tetrahedral semiconductors.<sup>2</sup> The hexagonal fault in cubic CsPbI<sub>3</sub> results in an even smaller SFE. This result is a consequence of the enhanced stability of 2H over 3C for CsPbI<sub>3</sub> at 0 K. The calculations confirm that stacking faults in halide perovskites have a small thermodynamic cost and are therefore likely to form.

To assess the electronic consequences, we have analyzed the band structure and alignments. The 2H sequence results in a larger indirect band gap relative to 3C, as expected. The two mixed models show intermediate behavior with a larger indirect band gap (3*c*8*h*) and a smaller direct band gap (2*h*9*c*). The band offsets were probed through analysis of the band-edge electron density, electrostatic potential, and core-level distributions. These unanimously confirm a preference for strong hole blocking by the stacking faults (Figure 2). The lower conduction band is always formed in the corner-sharing regions; however,

the upper valence band can be formed in the corner-sharing (for 2*h*9*c*) or face-sharing (for 3*c*8*h*) regions.

For the  $c$  region in the  $h$  structure, there is a staggered type-II band offset that results in selective trapping of electrons with a 0.07 eV potential well. For the  $h$  region in the  $c$  structure, the valence band exhibits a much larger shift (0.26 eV) compared to the conduction band (0.001 eV), which would result in a strong hole-blocking effect but no electron trapping.

Significant polarization is observed at the boundaries of the polytype regions, as evidenced by the distorted Pb 6s (valence band) and Pb 6p (conduction band) charge density, as well as the displacements of Cs atoms, in Figure 2. Such interface dipoles could be large enough to change the nature of the band offset type and behavior, depending on the size and orientation of the polytype arrangement on each side of the junction. We note that the  $P6_3mc$  space group of 2H is noncentrosymmetric and piezoelectric; the properties of such junctions will be sensitive to crystal strain.

Our central conclusion is that although corner-sharing and face-centered halide perovskite polytypes are well studied, they represent two extremes. A spectrum of structures exist in between them with more complex stacking sequences, as evidenced by recent reports.<sup>13</sup> We have shown that hexagonal inclusions can readily form in halide perovskite crystals and their primary effect will be to suppress hole transport across grains. Crystal engineering to obtain mixtures of corner- and face-

sharing octahedral networks opened an avenue to obtain new functionality in oxide perovskites.<sup>14</sup> Building on progress in high-resolution microscopy of halide perovskites,<sup>6,15</sup> deeper experimental and theoretical investigations into polytype stability and stacking fault behavior, including the role of chemical composition, is warranted.

## AUTHOR INFORMATION

### Corresponding Author

Aron Walsh – Department of Materials, Imperial College London, London SW7 2AZ, U.K.; Department of Materials Science and Engineering, Yonsei University, Seoul 03722, Korea;  
✉ [orcid.org/0000-0001-5460-7033](https://orcid.org/0000-0001-5460-7033); Email: [a.walsh@imperial.ac.uk](mailto:a.walsh@imperial.ac.uk)

### Authors

Ji-Sang Park – Department of Physics, Kyungpook National University, Daegu 41566, Korea; ✉ [orcid.org/0000-0002-1374-8793](https://orcid.org/0000-0002-1374-8793)

Zhenzhu Li – College of Energy, Soochow Institute for Energy and Materials InnovationS (SIEMIS), Soochow University, Suzhou 215006, China

Jacob N. Wilson – Department of Materials, Imperial College London, London SW7 2AZ, U.K.

Wan-Jian Yin – College of Energy, Soochow Institute for Energy and Materials InnovationS (SIEMIS), Soochow University, Suzhou 215006, China; ✉ [orcid.org/0000-0003-0932-2789](https://orcid.org/0000-0003-0932-2789)

Complete contact information is available at:

<https://pubs.acs.org/10.1021/acsenerylett.0c01124>

### Notes

The authors declare no competing financial interest. Structural models were generated for the two stacking faults starting from the crystal structure of pristine cubic CsPbI<sub>3</sub>. The structure models and the code used to generate them are available in an online repository at <http://doi.org/10.5281/zenodo.3878743>.

## ACKNOWLEDGMENTS

We acknowledge the assistance of Caroline Boule and Samantha Hood in the early stages of the project. We are grateful to the UK Materials & Molecular Modelling Hub for resources, funded by EPSRC (EP/P020194/1). Via our membership of the UK's HPC Materials Chemistry Consortium (EP/L000202, EP/R029431), this work used the ARCHER Supercomputer. This work was also supported by the National Research Foundation of Korea (NRF) grant funded by the Korean government (MSIT) (No. NRF-2020R1F1A1053606).

## REFERENCES

- (1) Yeh, C.-Y.; Lu, Z.; Froyen, S.; Zunger, A. Zinc-blende–wurtzite polytypism in semiconductors. *Phys. Rev. B: Condens. Matter Mater. Phys.* **1992**, *46*, 10086.
- (2) Yoo, S.-H.; Butler, K. T.; Soon, A.; Abbas, A.; Walls, J. M.; Walsh, A. Identification of critical stacking faults in thin-film CdTe solar cells. *Appl. Phys. Lett.* **2014**, *105*, 062104.
- (3) Eperon, G. E.; Paterno, G. M.; Sutton, R. J.; Zampetti, A.; Haghighirad, A. A.; Cacialli, F.; Snaith, H. J. Inorganic caesium lead iodide perovskite solar cells. *J. Mater. Chem. A* **2015**, *3*, 19688–19695.
- (4) Gratia, P.; Zimmermann, I.; Schouwink, P.; Yum, J.-H.; Audinot, J.-N.; Sivula, K.; Wirtz, T.; Nazeeruddin, M. K. The many faces of mixed ion perovskites: unraveling and understanding the crystallization process. *ACS Energy Lett.* **2017**, *2*, 2686–2693.

(5) Beecher, A. N.; Semonin, O. E.; Skelton, J. M.; Frost, J. M.; Terban, M. W.; Zhai, H.; Alatas, A.; Owen, J. S.; Walsh, A.; Billinge, S. J. Direct observation of dynamic symmetry breaking above room temperature in methylammonium lead iodide perovskite. *ACS Energy Lett.* **2016**, *1*, 880–887.

(6) Rothmann, M. U.; Li, W.; Zhu, Y.; Bach, U.; Spiccia, L.; Etheridge, J.; Cheng, Y.-B. Direct observation of intrinsic twin domains in tetragonal CH<sub>3</sub>NH<sub>3</sub>PbI<sub>3</sub>. *Nat. Commun.* **2017**, *8*, 14547.

(7) Perdew, J. P.; Ruzsinszky, A.; Csonka, G. I.; Vydrov, O. A.; Scuseria, G. E.; Constantin, L. A.; Zhou, X.; Burke, K. Restoring the density-gradient expansion for exchange in solids and surfaces. *Phys. Rev. Lett.* **2008**, *100*, 136406.

(8) Kresse, G.; Furthmüller, J. Efficient iterative schemes for ab initio total-energy calculations using a plane-wave basis set. *Phys. Rev. B: Condens. Matter Mater. Phys.* **1996**, *54*, 11169–11186.

(9) Park, J.-S.; Calbo, J.; Jung, Y.-K.; Whalley, L. D.; Walsh, A. Accumulation of Deep Traps at Grain Boundaries in Halide Perovskites. *ACS Energy Lett.* **2019**, *4*, 1321–1327.

(10) Sutton, R. J.; Filip, M. R.; Haghighirad, A. A.; Sakai, N.; Wenger, B.; Giustino, F.; Snaith, H. J. Cubic or orthorhombic? Revealing the crystal structure of metastable black-phase CsPbI<sub>3</sub> by theory and experiment. *ACS Energy Lett.* **2018**, *3*, 1787–1794.

(11) Kye, Y.-H.; Yu, C.-J.; Jong, U.-G.; Ri, K.-C.; Kim, J.-S.; Choe, S.-H.; Hong, S.-N.; Li, S.; Wilson, J. N.; Walsh, A. Vacancy-driven stabilization of the cubic perovskite polymorph of CsPbI<sub>3</sub>. *J. Phys. Chem. C* **2019**, *123*, 9735–9744.

(12) Travis, W.; Glover, E.; Bronstein, H.; Scanlon, D.; Palgrave, R. On the application of the tolerance factor to inorganic and hybrid halide perovskites: a revised system. *Chem. Sci.* **2016**, *7*, 4548–4556.

(13) Dang, H. X.; et al. Multi-cation synergy suppresses phase segregation in mixed-halide perovskites. *Joule* **2019**, *3*, 1746–1764.

(14) Fop, S.; McCombie, K. S.; Wildman, E. J.; Skakle, J. M.; McLaughlin, A. C. Hexagonal perovskite derivatives: a new direction in the design of oxide ion conducting materials. *Chem. Commun.* **2019**, *55*, 2127–2137.

(15) Zhou, Y.; Sternlicht, H.; Padture, N. P. Transmission electron microscopy of halide perovskite materials and devices. *Joule* **2019**, *3*, 641–661.